JACC: CARDIOVASCULAR IMAGING VOL. 3, NO. 8, 2010

ISSN 1936-878X/$36.00
PUBLISHED BY ELSEVIER INC. DOI:10.1016/j.jcmg.2010.03.013

CVN Interview

ORIGINAL RESEARCH

Intravascular and Extravascular Microvessel Formation in Chronic Total Occlusions

A Micro-CT Imaging Study

Nigel R. Munce, PhD,* Bradley H. Strauss, MD, PhD,†‡ Xiuling Qi, PhD,† Max J. Weisbrod,† Kevan J. Anderson, BEng,* General Leung, MSc,* John D. Sparkes, MSc,† Julia Lockwood,† Ronen Jaffe, MD,† Jagdish Butany, MD,§ Aaron A. Teitelbaum, MD, MSc,† Beiping Qiang, MD, PhD,† Alexander J. Dick, MD,† Graham A. Wright, PhD*†

Toronto, Ontario, Canada

OBJECTIVES The purpose of this study was to characterize the 3-dimensional structure of intravascular and extravascular microvessels during chronic total occlusion (CTO) maturation in a rabbit model.

BACKGROUND Intravascular microchannels are an important component of a CTO and may predict guidewire crossability. However, temporal changes in the structure and geographic localization of these microvessels are poorly understood.

METHODS A total of 39 occlusions were created in a rabbit femoral artery thrombin model. Animals were sacrificed at 2, 6, 12, and 24 weeks (n ≥8 occlusions per time point). The arteries were filled with a low viscosity radio-opaque polymer compound (Microfil) at 150 mm Hg pressure. Samples were scanned in a micro-computed tomography system to obtain high-resolution volumetric images. Analysis was performed in an image processing package that allowed for labeling of multiple materials.

RESULTS Two distinct types of microvessels were observed: circumferentially oriented "extravascular" and longitudinally oriented "intravascular" microvessels. Extravascular microvessels were evident along the entire CTO length and maximal at the 2-week time point. There was a gradual and progressive reduction in extravascular microvessels over time, with very minimal microvessels evident beyond 12 weeks. In contrast, intravascular microvessel formation was delayed, with peak vascular volume at 6 weeks, followed by modest reductions at later time points. Intravascular microvessel formation was more prominent in the body compared with that in the proximal and distal ends of the CTO. Sharply angulated connections between the intravascular and extravascular microvessels were present at all time points, but most prominent at 6 weeks. At later time points, the individual intravascular microvessels became finer and more tortuous, although the continuity of these microvessels remained constant beyond 2 weeks.

CONCLUSIONS Differences are present in the temporal and geographic patterns of intravascular and extravascular microvessel formation during CTO maturation. (J Am Coll Cardiol Img 2010;3: 797–805) © 2010 by the American College of Cardiology Foundation

From the *Department of Medical Biophysics, University of Toronto, †Schulich Heart Programme, Sunnybrook Research Institute, Sunnybrook Health Sciences Centre, ‡McLaughlin Centre for Molecular Medicine, University of Toronto, and the §Department of Pathology, University Health Network, Toronto, Ontario, Canada. This study was funded by the Canadian Institute of Health Research.

Manuscript received July 15, 2009; revised manuscript received January 6, 2010, accepted March 1, 2010.

Chronic coronary artery occlusions are extremely common, occurring in about one-third to one-half of all coronary angiograms (1,2). In addition, ~1% of patients over the age of 60 have symptomatic occlusive peripheral arteries (3), and the incidence is particularly high among the diabetic population (~30%) (4). A chronic total occlusion (CTO) is defined as an angiographic occlusion (Thrombolysis In Myocardial Infarction [TIMI] flow grade ≤1) that is older than 3 months (5). Several studies have shown that successful revascularization of a coronary CTO corresponds to a reduction in symptoms (6) and improved left ventricular function (7). Despite the potential clinical benefits of percutaneous treatment of CTOs, these efforts are limited by difficulty in directing the guidewire across the CTO before balloon angioplasty (8,9).

See page 806

ABBREVIATIONS AND ACRONYMS

CTO = chronic total occlusion

IMV = intravascular microvessel volume

μCT = micro-computed tomography

While, by definition, a CTO lacks flow seen under angiography, previous studies have indicated that about 50% of CTOs have histological evidence of vascularity, and are in fact <99% occluded (10). Neovascularization within an occluded arterial segment may occur within the lumen or various layers of the vessel wall and result from distinct pathologic processes. The vasa vasorum are a network of small vessels located in the adventitia and the deeper layers of the tunica media that proliferate in response to injury (11,12). Intimal vessels are present within atherosclerotic plaques and could originate from the vasa vasorum as a response to inflammatory and hypoxic factors (13). In addition, recanalization microvessels resulting from reorganization of thrombus within the occlusion have been observed (10). These microvessels may be critical for successful guidewire crossing as the path of least resistance through the dense collagen of the occlusion (14).

Previous pathology studies (10,15) have described tissue composition within CTOs; however, information on the global architecture of an occlusion has been poorly understood. This knowledge deficit has been largely due to the limited number of histological cross-sections that can be processed and analyzed. Furthermore, it has been challenging to correlate these histological sections with the proximal end, body, and distal end of the occlusion. While imaging techniques can address some of these difficulties, they typically lack sufficient resolution to examine details, such as microvasculature, appropriately. One imaging modality that has been widely employed for high-resolution ex vivo imaging is micro-computed tomography (μCT) with spatial resolution on the order of 10 μm (16).

Recently, we reported on the maturational changes of CTOs in a rabbit femoral artery model, including the general pattern of intravascular microchannels within the CTO. In particular, we found differences in intravascular microchannel volume at different time points using magnetic resonance imaging and histology (17). This study, however, lacked sufficient spatial resolution on a global scale to investigate the evolution of the 3-dimensional morphology of microvessels in CTOs, particularly in relationship to the specific location within the CTO (proximal end, body, and distal end). It was also unclear to what extent the vessels from outside of the occluded artery interacted with those channels that appeared within the occluded lumen. Therefore, we sought to use μCT of contrast-perfused CTOs at different time points to investigate the evolution of the 3-dimensional microvasculature associated with a rabbit occlusion model.

METHODS

The occlusion model. Approval for experiments was obtained from Sunnybrook Hospital Animal Care Committee. Bilateral arterial occlusions were initiated in 28 male New Zealand white rabbits (Charles River Canada, St. Constant, Quebec) weighing 3.0 to 3.5 kg, as previously described (18). Briefly, a femoral artery segment was isolated and ligated at each end. The segment was then injected with ~0.1 ml (100 IU/ml) bovine thrombin solution, and then the proximal ligature was removed to allow blood to mix with the thrombin to create a thrombus. The distal ligature was maintained up to 60 min to ensure a persistent occlusion. Animals were then returned to their cage and fed a regular diet. Animals were sacrificed at 2, 6, 12, and 24 weeks (n ≥8 occlusions per time point) after creation of the CTO.

Contrast perfusion and imaging. A contrast X-ray angiogram (Fig. 1) was performed to verify the occlusion before sacrifice. After the angiogram, the catheter was withdrawn and intravenous heparin (1,000 units) was administered ~10 min before sacrifice to prevent blood coagulation in the microvasculature. Immediately after sacrifice, a syringe was inserted into the abdominal aorta and the tip

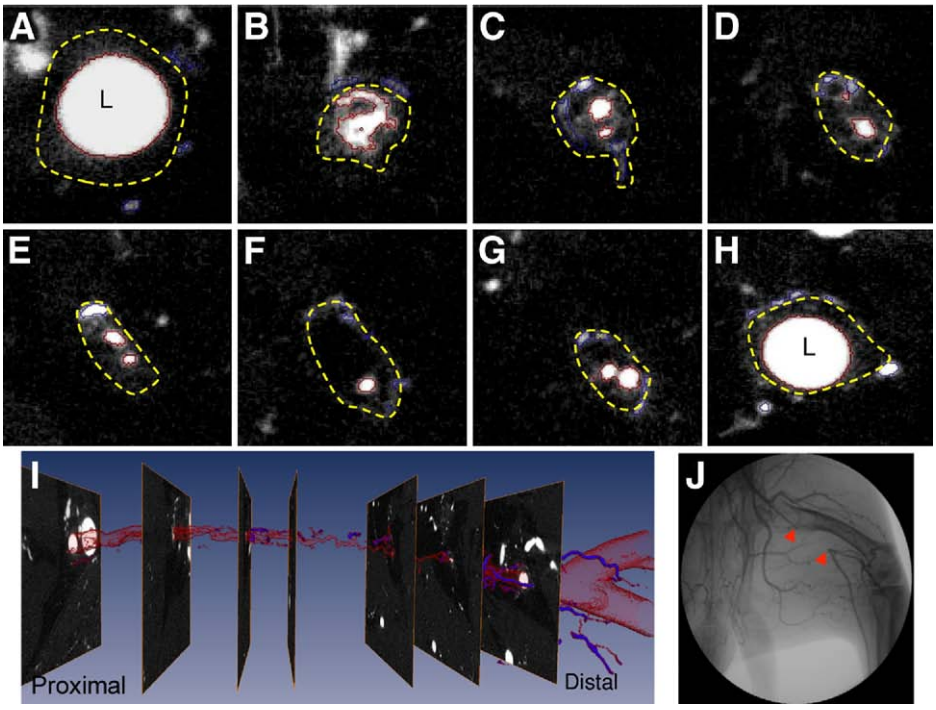

Figure 1. Micro-CT Axial Slices and Labeling Procedure

Micro-computed tomography (μ-CT) slices are shown from **(A)** proximal to **(H)** distal positions through the lesion and follow both the intravascular channels **(red)** and extravascular channels **(blue)**. The patent lumen is identified with the letter "L." The **dotted yellow line** represents the outer border of the artery. **(I)** Resulting volumes generated from the labeled materials and the location of the axial slices are shown. **(J)** Angiogram of a 12-week-old chronic total occlusion (**red arrowheads** identify the proximal and distal ends).

was tied in place with a ligature to prevent back flow. After an injection of 30 ml normal saline to flush blood from the main arterial system, Microfil (Flow Tech, Carver, Massachusetts) was injected at a pressure of 150 mm Hg as measured by a handheld manometer. The Microfil was given 1 h to set, then the femoral arteries were surgically removed and left in formalin for 48 h. Specimens were then embedded in 2% w/w agarose gel. The samples were imaged in a μCT system (MS-8, GE Medical Systems, London, Ontario) (16). Three-dimensional cone beam CT data sets were acquired in 2.5 h with 905 views and reconstructed at 14-μm resolution. An X-ray source of voltage 80 KVp and a beam current 90 mA was used.

Image analysis. The μCT volume was imported into image analysis software (Amira, Mercury Computer Systems, Chelmsford, Massachusetts). This software enables labeling of 2 distinct types of vasculature seen within the CTO: "intravascular" microvessels representing recanalization channels within the occluded lumen and media; and "extravascular" vessels, representing microvessels outside of the boundary of the arterial wall. Labeling of the intravascular microvessels was done by first identifying the patent vessel just before the occlusion; this vascular area was labeled with a software tool that acted as a seed-growing algorithm, propagating the intravascular region through connected regions in successive axial slices. A similar step was performed at the distal end. This seed-growing algorithm typically labeled all connected vasculature associated within the occluded artery segment.

To identify vessels that were extravascular, 2 methods were applied. First, extravascular channels could be directly identified at the proximal and distal ends as the small vessels surrounding the patent artery before the occlusion. These vessels were typically arranged in a circumferential ring around the patent vessel (as shown in Fig. 1A), and were labeled as a different material in Amira using a software tool that filled in homogenous areas and stopped when the pixel value changed abruptly. These circumferential vessels were labeled for each slice as they progressed into the occlusion. The circumferential geometry of these channels was used to define a border between the intravascular and extravascular vessels. This border was marked

on the screen as a reference, as shown in Figure 1A through 1H by the dotted yellow line. As we progressed through the axial slices of the occlusion, vessels that were arranged in a semicircular shape that fit on or outside of this border were labeled as extravascular. Second, at time points >2 weeks, sufficient contrast was consistently obtained between the tissue surrounding the artery and the artery itself. This contrast was enhanced at these later time points when there was an increasing relative amount of loose connective tissue surrounding the artery. In these slices, vessels that appeared on the border of loose connective tissue and the artery were labeled as extravascular. Intravascular channels, which crossed the arterial border, were relabeled as extravascular when they crossed that border. The outer boundary used to identify extravascular vessels across the length of the CTO was determined by the average diameter containing extravascular vessels surrounding the patent artery before the proximal end of the occlusion.

Labeling was performed by 2 independent readers (N.M. and M.W.) who were blinded to the time point. The results from each reader were averaged. The software package was used to color code and display the intravascular vessels red, and the extravascular vessels blue on an isosurface (Figs. 1 and 2). The software package also calculated the number of voxels in each axial slice that were identified as intravascular and extravascular. The start and end of the occlusion were defined as the axial slices in which the vessel lumen area, as measured by μCT, decreased by 90% compared with the patent artery. The CTO length was normalized to 500 arbitrary units using software (MATLAB, The Mathworks, Natick, Massachusetts) so that occlusions of different lengths could be compared. Based on our previous histological studies (17), minimal variation in the cross-sectional area of the occluded lumen was observed in animals at the same time point. Thus, for this work, occlusions were normalized to a standard length rather than both length and occluded lumen area. An averaged vascular distribution at each time point was obtained by averaging these normalized vascular distributions.

Continuity represents the cumulative length of the intravascular microvessels along the entire CTO length. Percent continuity was calculated by identifying all continuous segments (minimal length requirement 1 mm), and defining the percent "continuity" of the channels in a CTO as the sum of the lengths of all of these segments divided by the total length of the occlusion. Parallel intravascular microchannels that were observed to join together were counted as a single segment in the context of this continuity measurement.

Average intravascular microvessel diameter was also calculated for each time point by assuming that there was typically a single channel in an imaging

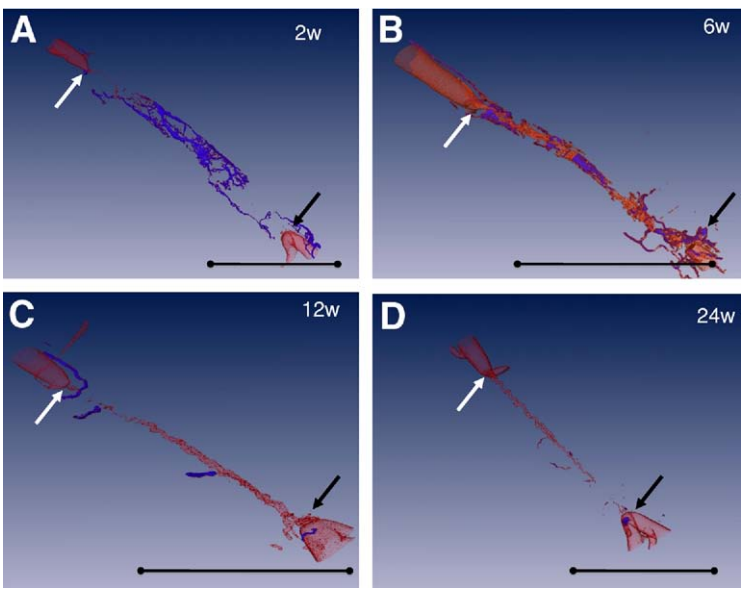

Figure 2. Progression of an Arterial Occlusion Over Time

Progression of microvasculature at **(A)** 2 weeks, **(B)** 6 weeks, **(C)** 12 weeks, and **(D)** 18 to 24 weeks. **White arrows** represent the proximal end; **black arrows** represent the distal end. Intravascular channels are shown in **red**; extravascular channels are shown in **blue**.

slice and approximating that the shape of the microchannel was a square in that slice.

Communicating channels were defined as points in which an intravascular channel crossed the defined border between the intravascular and extravascular channels. These events were counted by scrolling through all of the axial slices of each occlusion and counting the number of such incidences. The number of these events was averaged for each time point.

Statistical analysis. Analysis of variance for microvascular volumes, continuity, number of communicating channels, number of microchannel segments, diameter of microchannels, and occlusion length was performed in SAS version 9.0 (SAS Institute, Cary, North Carolina) using the general linear model procedure to compare mean responses at each of the 4 time points. Since the number of occlusions varied slightly among the different time points, least squares means were calculated for each time point; the mean and standard error of the mean (SEM) were calculated for each time point. Probabilities for comparisons between means were adjusted for multiple comparisons by the method of Tukey-Kramer. A p value of < 0.05 was considered significant.

RESULTS

Thirty-nine occlusions were successfully created in 28 rabbits. Six of these occlusions were not analyzable because of poor filling with Microfil (n = 3) and occlusion length <1 mm (n = 3). This gave an overall number of data points from each time point as follows: n = 9, 2-week-old occlusions from 7 rabbits; n = 8, 6-week-old occlusions from 5 rabbits; n = 8, 12-week-old occlusions from 6 rabbits; n = 8, 24-week-old occlusions from 6 rabbits. The average interobserver variability of the 2 trained readers in the analysis of the intravascular microvessel volume (IMV) was 10.2%.

Typical 3-dimensional microvascular volumes at 2, 6, 12, and 24 weeks are displayed in Figure 2A through 2D. The proximal end of the CTO typically was at the origin of a branching collateral, and the distal end was reconstituted at a bifurcation of the femoral artery. The average length of the occlusion was 18.1 ±1.0 mm at 2 weeks, 12.2 ± 1.2 mm at 6 weeks, 15.9 ± 1.2 mm at 12 weeks, and 14.4 ± 1.1 mm at 24 weeks. The overall p value for the occlusions lengths comparing weeks 2 to 24 was calculated as p = 0.006. The volumetric images showed a progression from a poorly defined proximal end at the early 2-week time point (Fig. 2A) to a tapered corkscrew-like pattern at both the proximal and distal ends of the occlusion at later time points (Fig. 2B to 2D). Rotational movies of these volumes are available as online supplemental media (Online Videos 1, 2, 3, and 4), which allow for better appreciation of the overall structure of the occlusion.

Extravascular vessel formation. Extravascular vessels appeared as circumferentially oriented vessels on the outer surface of the occluded artery. These vessels were most predominant at the 2-week time point, appearing as a fine network of vessels surrounding the artery (Fig. 2A, blue color). As the occlusion age increased, these vessels were markedly decreased in number, although larger in size compared with the 2-week time point (Fig. 2B to 2D). There was a significant reduction in the total extravascular volume with age (p = 0.0024 comparing 2-week vs. 24-week-old CTOs) (Fig. 3B).

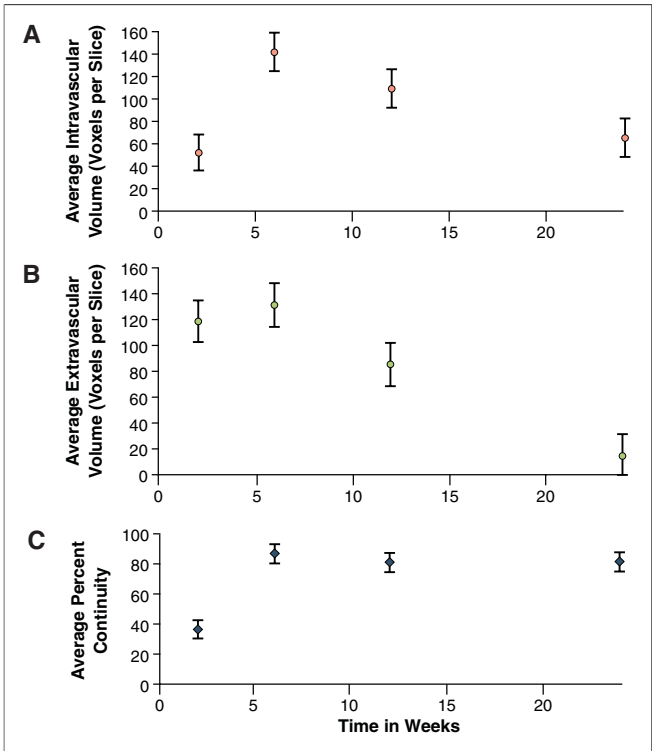

Figure 3. Total Intravascular and Extravascular Microchannel Volume and Continuity

(A) The evolution of the total intravascular microvessel volume in an arterial occlusion is shown over time, as measured by micro-computed tomography. **(B)** The corresponding changes seen in the extravascular microvessels are shown over the same time frame. The graph shown in **(C)** illustrates the evolution of the continuity of the microchannels in the occlusion as a function of time.

The distribution of the extravascular microvessels at 2 weeks was characterized by 2 broad peaks (Fig. 4B) within the body of the occlusion. At the 6-week time point, there was a shift of this distribution toward the proximal end. Although there were few extravascular microvessels present beyond the 6 week time point, these microvessels were evenly distributed along the length of the CTO.

Intravascular microchannel volume. There was a marked increase (2.7 times increase) in the total IMV observed between the 2- and 6-week time points ($p = 0.003$) as shown in Figure 3A. The overall IMV then progressively declined by a factor of 2.1 between 6 and 24 weeks ($p < 0.017$) (Fig. 3A), primarily as a result of a decrease in diameter of the vessels. The spatial distribution of these intravascular channels, which was normalized to the length of the occlusion for each time point, is shown in Figure 4A. We observed a predominance of IMV within the central body of the CTO at the 6-week time point as compared with the proximal and distal end regions of the CTO (Fig. 4A). At later time points, there was a prominent reduction in the IMV within the central body of the CTO, with relative sparing of IMV at the proximal and distal end regions (Fig. 4A).

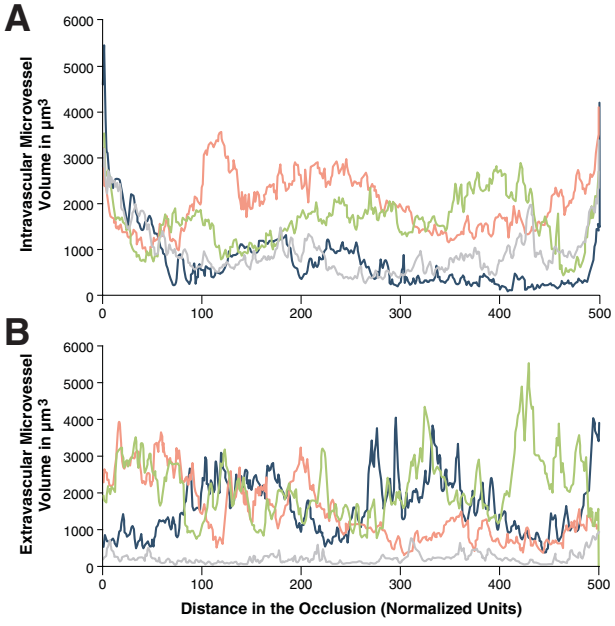

Figure 4. Averaged Distribution of Intravascular and Extravascular Microchannel Volume

Average intravascular **(A)** and extravascular **(B)** microvessel volume as a function of position within the occlusion for several time points. Distance within the occlusion is normalized by total occlusion length so that each occlusion is 500 units long. **Dark gray line** indicates 2 weeks; **orange line** indicates 6 weeks; **green line** indicates 12 weeks; **light gray line** indicates 24 weeks.

Continuity of microchannels. There was minimal continuity of the intravascular microchannels at the 2-week time point. However, at all later time points (≥6 weeks), an average continuity of 85% was observed (Fig. 4C), meaning that 85% of the length of the occlusion could be traversed by following such a microchannel. There were significant differences in continuity of the intravascular microvessels between 2 weeks and all later time points ($p < 0.0002$). Interestingly, the intravascular channels within the occlusion were typically composed of 1 to 3 different channel segments. These segments were often connected to either the proximal and/or distal end of the occlusion. The average length of these segments was significantly higher ($p < 0.05$) at the later time points (7.0 ± 1.3 mm at 6 weeks, 8.5 ± 1.3 mm at 12 weeks, and 6.3 ± 1.2 mm at 24 weeks) compared with the 2-week time point (3.5 ± 1.1 mm).

Intravascular microchannel diameter. There was a significant increase ($p < 0.03$) in the average diameter of the intravascular microchannels between the 2- and 6-week time points (115 ± 15 μm at 2 weeks, 198 ± 16 μm at 6 weeks). No significant difference ($p = 0.65$) was seen between the microvessels diameters at 6 and 12 weeks (172 ± 16 μm at 12 weeks). As the occlusion aged, however, the microvessel diameter decreased (134 ± 16 μm at 24 weeks), and a significant difference was seen comparing the diameters of the microvessels at the 6- and 24-week time points ($p = 0.03$).

Communications between intravascular and extravascular channels. Communicating channels were observed at all time points (Fig. 5A), with a peak number at the 6-week time point, which gradually decreased over time (Fig. 5C). There were significantly fewer communicating channels at the 2-week time point compared with the 6-week time point ($p = 0.02$). However, there were no significant differences in the number of communicating channels comparing weeks 6 through 24 ($p > 0.15$). These communicating channels exited at acute angles (Fig. 5D).

DISCUSSION

In this study, we report on the evolution of the 3-dimensional morphology of microvessels in a CTO model. We also performed a detailed analysis of the maturation of these microvessels according to

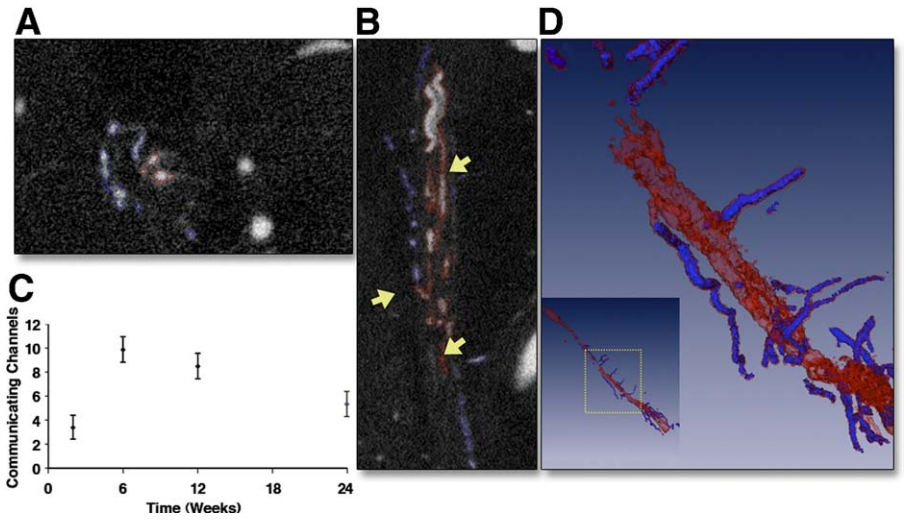

Figure 5. Communicating Vessels in Arterial Occlusions

(A) A micro-computed tomography slice showing intravascular microvessels **(red)** communicating with extravascular microvessels in the arterial wall **(blue)**. **(B)** Longitudinal slice through the occlusion showing communicating channels **(yellow arrows)**. **(C)** Number of such channels as a function of the occlusion age. **(D)** Volume-rendered image of a 12-week chronic total occlusion showing several extravascular microvessels **(blue)** communicating with intravascular vessels. **Inset image** shows wide field view of the chronic total occlusion, with the proximal entrance located in the upper left-hand corner; the **yellow box** illustrates the magnified region shown in the main image.

location within the vessel layers (intravascular versus extravascular) and specific distribution along the CTO (proximal, central body, distal).

The primary finding of this work was that a large rise in extravascular vessels surrounding the occluded artery occurred at early time points, which was followed by a statistically significant increase in intravascular vessels within the central body of the occlusion. The temporal and geographic pattern of microvessel formation and the presence of connecting microvessels suggested that the extravascular vessels may initiate formation of the intravascular channels within the center of the occlusion, as was evident in the distribution of intravascular channels along the length of the occlusion. The stimulus for the increased neovasculature observed within the center body of the lesion may be due to greater hypoxia in this region, particularly at these early time points. These channels may lead to a significantly smaller occlusion length at the 6-week time point as compared to the acute 2-week period.

As the occlusion reaches the age of 6 weeks, neovascularization also occurred at both the proximal and distal ends of the lesion. This process at the proximal end has previously been correlated with the presence of the tapered entrances similar to those seen in angiography (8). The mechanism of formation of the vessels from the proximal and distal ends is uncertain, but could be related to ingrowing recanalization channels from the adjacent nonoccluded segments and/or the effects of specialized circulating cells, as has been observed in venous thrombi (19). These tapered entrances eventually connected to the microvasculature in the center of the lesion—resulting in long continuous channels through the lesion.

However, at later time points beyond 6 weeks, there was a reduction in the size and number of central intravascular microchannels, suggesting that many of the vessels in this region become nonfunctional. As the occlusion further ages, only a single narrow intravascular channel was present. While this channel may provide a pathway through the CTO, its small diameter and tortuous nature would be challenging to cross with guidewires, and make it susceptible to occluding as well. The increase in occlusion length associated with later time points may be due to the occlusion of these microchannels.

These observations are in agreement with the general trends that we have reported in a previous study involving histological evaluation of microchannels (15). In that work, we also saw a peak in microchannel vascularity at the 6-week time point that regressed as the occlusion aged. That previous study, however, was not able to provide the detailed structure and topographic information along the length of the occlusion as we were limited to several histological slices.

Study limitations. The CTO model differed from the clinical case primarily because of its lack of atherosclerotic substrate. This substrate is often associated with an area of increased angiogenesis within the plaque; therefore, investigating the interaction of these vessels with those associated with the CTO remains an outstanding issue. The absence of calcification in the arterial wall in this model may also have significant implications for the architecture of the occlusion. The current work suggests that vessels from outside of the occlusion play a key role in the development of intravascular microchannels; the presence of calcification in the artery's medial wall may affect this process. Furthermore, due to the current requirements of ex vivo tissue for performing μCT studies, individual animals could not be followed up serially. This limitation results in the need for us to compare different animals at different time points, thus increasing variability. Newer μCT systems coupled with blood-pool contrast agents may be able to address this challenge in the future (20).

CONCLUSIONS

The results of this study indicate that, within the initial 12 weeks, microvessels are continuous across large segments of the occlusion. While the typical diameter of the intravascular channels that we observed in this study at 6 and 12 weeks was less than that of a standard 0.014-inch (355-μm) guidewire, it is likely that the presence of the microvessel alters the local tissue compliance. Thus, the guidewire may still follow the path of a microvessel, as it is the path of least resistance through the occlusion. The smaller number and diameter of intravascular microchannels in older CTOs, which correspond to lower guidewire crossing rates in percutaneous revascularization (8), provides a rationale for targeting intravascular angiogenesis to facilitate endovascular strategies.

It is also important to recognize that the presence of communicating channels between extravascular and intravascular networks may contribute to diversion of guidewires into the extravascular space. The images we obtained of the communicating channels suggest that the majority of these channels exit the lesion at an angle close to 90° to the path of the artery, and hence, it is unlikely that the guidewire would make such a sharp, sudden turn. These channels, however, may explain some of the dissections that occur during guidewire manipulations, and when operators employ devices that follow the "path of least resistance" through a CTO (21,22).

Recent work has suggested that conventional fluoroscopy can be used to build up 3- dimensional images of microchannels within CTOs (23). Although the authors of that work were not able to resolve the complex 3-dimensional structure of the microchannels, they also reported seeing highly continuous channels in CTOs, which may be important predictors of procedural success. Further development of these imaging techniques, particularly the ability to identify points in which channels exit the lesion, may potentially improve planning and intraprocedural guidance of angioplasty procedures.

Reprint requests and correspondence: Dr. Nigel Munce, Sunnybrook Health Sciences Centre, 2075 Bayview Avenue, Room S612, Toronto, Ontario M4N 3M5, Canada. *E-mail: nigel.munce@gmail.com.*

REFERENCES

1. Kahn JK. Angiographic suitability for catheter revascularization of total coronary occlusions in patients from a community hospital setting. Am Heart J 1993;126:561–4.
2. Christofferson RD, Lehmann KG, Martin GV, Every N, Caldwell JH, Kapadia SR. Effect of chronic total coronary occlusion on treatment strategy. Am J Cardiol 2005;95:1088–91.
3. Criqui MH, Fronek A, Barrett-Connor E, Klauber MR, Gabriel S, Goodman D. The prevalence of peripheral arterial disease in a defined population. Circulation 1985;71:510–5.
4. Andrade JL, Schlaad SW, Koury Junior A, Van Bellen B. Prevalence of lower limb occlusive vascular disease in outclinic diabetic patients. Int Angiol 2004;23:134–8.
5. Stone GW, Kandzari DE, Mehran R, et al. Percutaneous recanalization of chronically occluded coronary arteries: a consensus document: part I. Circulation 2005;112:2364–72.
6. Olivari Z, Rubartelli P, Piscione F, et al. Immediate results and one-year clinical outcome after percutaneous coronary interventions in chronic total occlusions: data from a multicenter, prospective, observational study (TOAST-GISE). J Am Coll Cardiol 2003;41:1672–8.
7. Appleton DL, Abbate A, Biondi-Zoccai GG. Late percutaneous coronary intervention for the totally occluded infarct-related artery: a meta-analysis of the effects on cardiac function and remodeling. Catheter Cardiovasc Interv 2008;71:772–81.
8. Puma JA, Sketch MH Jr., Tcheng JE, et al. Percutaneous revascularization of chronic coronary occlusions: an overview. J Am Coll Cardiol 1995;26:1–11.
9. Noguchi T, Miyazaki MS, Morii I, Daikoku S, Goto Y, Nonogi H. Percutaneous transluminal coronary angioplasty of chronic total occlusions. Determinants of primary success and long-term clinical outcome. Catheter Cardiovasc Interv 2000;49:258–64.
10. Srivatsa SS, Edwards WD, Boos CM, et al. Histologic correlates of angiographic chronic total coronary artery occlusions: influence of occlusion duration on neovascular channel patterns and intimal plaque composition. J Am Coll Cardiol 1997;29:955–63.

11. Kwon HM, Sangiorgi G, Ritman EL, et al. Adventitial vasa vasorum in balloon-injured coronary arteries: visualization and quantitation by a microscopic three-dimensional computed tomography technique. J Am Coll Cardiol 1998;32:2072–9.
12. Cheema AN, Hong T, Nili N, et al. Adventitial microvessel formation after coronary stenting and the effects of SU11218, a tyrosine kinase inhibitor. J Am Coll Cardiol 2006;47:1067–75.
13. Luque A, Turu M, Juan-Babot O, et al. Overexpression of hypoxia/inflammatory markers in atherosclerotic carotid plaques. Front Biosci 2008;13:6483–90.
14. Strauss BH, Segev A, Wright GA, et al. Microvessels in chronic total occlusions: pathways for successful guidewire crossing? J Interv Cardiol 2005; 18:425–36.
15. Katsuragawa M, Fujiwara H, Miyamae M, Sasayama S. Histologic studies in percutaneous transluminal coronary angioplasty for chronic total occlusion: comparison of tapering and abrupt types of occlusion and short and long occluded segments. J Am Coll Cardiol 1993;21:604–11.
16. Marxen M, Thornton MM, Chiarot CB, et al. MicroCT scanner performance and considerations for vascular specimen imaging. Med Phys 2004; 31:305–13.
17. Jaffe R, Leung G, Munce NR, et al. Natural history of experimental arterial chronic total occlusions. J Am Coll Cardiol 2009;53:1148–58.
18. Strauss BH, Goldman L, Qiang B, et al. Collagenase plaque digestion for facilitating guide wire crossing in chronic total occlusions. Circulation 2003;108:1259–62.
19. Modarai B, Burnand KG, Sawyer B, Smith A. Endothelial progenitor cells are recruited into resolving venous thrombi. Circulation 2005;111: 2645–53.
20. Detombe SA, Ford NL, Xiang F, Lu X, Feng Q, Drangova M. Longitudinal follow-up of cardiac structure and functional changes in an infarct mouse model using retrospectively gated micro-computed tomography. Invest Radiol 2008;43:520–9.
21. Loli A, Liu R, Pershad A. Immediate- and short-term outcome following recanalization of long chronic total occlusions (> 50 mm) of native coronary arteries with the Frontrunner catheter. J Invasive Cardiol 2006;18:283–5.
22. Melzi G, Cosgrave J, Biondi-Zoccai GL, et al. A novel approach to chronic total occlusions: the crosser system. Catheter Cardiovasc Interv 2006;68: 29–35.
23. Dvir D, Assali A, Kornowski R. Percutaneous coronary intervention for chronic total occlusion: novel 3-dimensional imaging and quantitative analysis. Catheter Cardiovasc Interv 2008;71:784–9.

Key Words: chronic total occlusions ■ micro-computed tomography ■ microchannels ■ interventional cardiology.

APPENDIX

For supplemental Videos 1 to 4, please see the online version of this article.